

Skin-Friction and Forced Convection from an Isothermal Rough Plate

Aubrey G. Jaffer
agj@alum.mit.edu

Abstract

Presented are new correlations for skin-friction and forced convection from an isothermal plate having root-mean-squared height-of-roughness ε_q . Corresponding to Prandtl and Schlichting’s “fully-developed roughness” region, the skin-friction correlation is independent of Reynolds number; the convection correlation is a linear function of Reynolds number (versus an exponent of 4/5 for turbulent convection from a smooth plate).

$$f_c = \frac{1}{16 [\log_{10} \frac{\varepsilon_q}{L}]^2} \quad \text{Nu} = \frac{\text{Re Pr}^{1/3}}{32 [\log_{10} \frac{\varepsilon_q}{L}]^2}$$

Measurements taken of a plate having precisely 3 mm of roughness match the convection correlation within 3% at Reynolds numbers from 5000 to 50000. A formula addressing the transition from fully-rough turbulent to smooth turbulent convection for this bi-level test plate matches those measurements within 2% from Re=5000 to 80000.

Convection measurements of a bi-level plate having 1.03 mm of roughness are within the expected measurement uncertainties of the transition formula.

An analysis of sand-roughness finds that its relation to root-mean-squared height-of-roughness is non-linear. The resulting scale error explains discrepancies between the Prandtl and Schlichting formula, two recent papers, and the results presented here.

These new correlations and measurements imply a threefold tighter upper bound for the height of admissible-roughness than is given in Schlichting’s book *Boundary-layer theory*.

Keywords: skin-friction; forced convection; roughness; sand-roughness; admissible-roughness

Table of Contents

<i>Introduction</i>	2
<i>Prior Work</i>	2
<i>Skin-Friction and Convection</i>	3
<i>Pipe-Plate Analogy</i>	3
<i>Rough to Smooth Turbulence Transition</i>	6
<i>Sand Roughness</i>	9
<i>Admissible Roughness</i>	11
<i>Forced Convection Results</i>	12
<i>Directions for Further Work</i>	13
<i>Conclusions</i>	13
<i>References</i>	13

1. Introduction

Convection from a rough surface is important in modeling weather and the thermal behavior of buildings. The related phenomenon of skin-friction has wide application to the fluid dynamics of vehicles and turbines.

Most investigations of fluids flowing on rough surfaces have focused on the interior of pipes and ducts. These do not require a wind tunnel or water tank to operate, greatly simplifying most aspects of measurement.

The practice for quantifying roughness has primarily been by matching measured friction factors from pipes with Nikuradse’s “sand-roughness” experiments from the 1930s.

It would be desirable to calculate rough convection, and convection from plates in particular, from topographic measurements of roughness. This investigation establishes new skin-friction and forced-convection correlations driven by measurement of forced convection from plates having precisely machined height-of-roughness as described in *Convection Measurement Apparatus and Methodology*[1].

Section 5, “Rough to Smooth Turbulence Transition” can be skipped; its analysis was needed in order to make sense of measurements of the 1 mm roughness plate.

The analysis in Section 6, “Sand Roughness”, is to support comparisons with prior work.

2. Prior Work

In 1934 Prandtl and Schlichting published *Das Widerstandsgesetz rauher Platten (The Resistance Law for Rough Plates*[2]) which brilliantly infers the relation for skin-friction resistance for rough plates from their analysis of Nikuradse’s measurements of sand glued inside pipes. In *Boundary-layer theory*[3] Prandtl and Schlichting give a formula for fully rough (large Re) total skin-friction coefficient for a rough flat plate:

$$c_f = \left(1.89 + 1.62 \log_{10} \frac{l}{k_S}\right)^{-2.5} \quad 10^2 < L/k_S < 10^6 \quad (1)$$

In *On the Skin Friction Coefficient for a Fully Rough Flat Plate*[4], Mills and Hang present a formula they claim to be more accurate on the local skin-friction measurements done by Pimenta, Moffat, and Kays[5]. Their total skin-friction formula is:

$$C_D = \left(2.635 + 0.618 \ln \frac{L}{k_S}\right)^{-2.57} \quad (2)$$

Putting these formulas into similar form:

$$c_f = 0.299 \left(\log_{10} \frac{14.68 \cdot l}{k_s}\right)^{-2.5} \quad C_D = 0.404 \left(\log_{10} \frac{71.1 \cdot L}{k_S}\right)^{-2.57}$$

The roughness in both papers is reported in Nikuradse’s sand-roughness metric k_S , the height of “coarse and tightly placed roughness elements such as for example coarse sand grains glued on the surface”. Prandtl and Schlichting[2] gives the parameters of Nikuradse’s sand coatings:

k_S	grains/cm ²	k_S^{-2}
.08 cm	150	156.25/cm ²
.04 cm	590	625/cm ²
.02 cm	1130	2500/cm ²
.01 cm	4600	10000/cm ²

Table 1 Nikuradse’s sand coatings

A correlation retaining its validity when all lengths are scaled by the same factor is a central tenet of fluid-dynamics theory. Because their packing densities scale as the inverse square of grain size, the .08 cm and .04 cm sand coatings should scale correctly as long as the glue thickness is proportional to grain size. Similarly the .02 cm and .01 cm sand coatings should scale.

The two coarsest coatings (largest k_S values) had packing densities slightly less than a square packing. The other two had packing densities less than half that of a square packing. But comparing the .02 cm and .04 cm sand coatings, their packing density ratio is nearly 1:2, not 1:4. Thus formulas (1) and (2) will have incorporated a scale error (between measurements of large and small k_S) and should not be applied to L/k_S values much larger than 1000 (507 is the largest rough pipe R/k_S value in Schlichting[3] Fig. 20.18). Section 6 compares these formulas with the present work.

3. Skin-Friction and Convection

The ratio of the mean height-of-roughness in a pipe to the pipe diameter (its characteristic-length) affects the friction factor used to compute pressure drops in flows through pipes. The Chilton and Colburn J-factor analogy (3) relates friction factors to turbulent forced convective heat transfer.

$$\text{Nu} = \frac{f}{2} \text{Re} \text{Pr}^{1/3} \quad (3)$$

The accepted correlation for turbulent convection from a smooth flat plate is:

$$\text{Nu} = 0.037 \text{Re}^{4/5} \text{Pr}^{1/3} \quad (4)$$

Combining correlation (4) with the Chilton and Colburn J-factor analogy (3) and solving for the Darcy friction factor $f_D = 4f$ yields:

$$f_D = 8 \cdot 0.037 \text{Re}^{-1/5} \quad (5)$$

4. Pipe-Plate Analogy

For turbulent flow, $\text{Re} > 2300$, f_D in a pipe can be modeled by the Colebrook-White equation (6):

$$\begin{aligned} \frac{1}{\sqrt{f_D}} &= 1.74 - 2 \log_{10} \left(\frac{k_S}{R} + \frac{18.7}{\text{Re} \sqrt{f_D}} \right) \\ &= -2 \log_{10} \left(\frac{k_S}{7.41 R} + \frac{2.52}{\text{Re} \sqrt{f_D}} \right) \end{aligned} \quad (6)$$

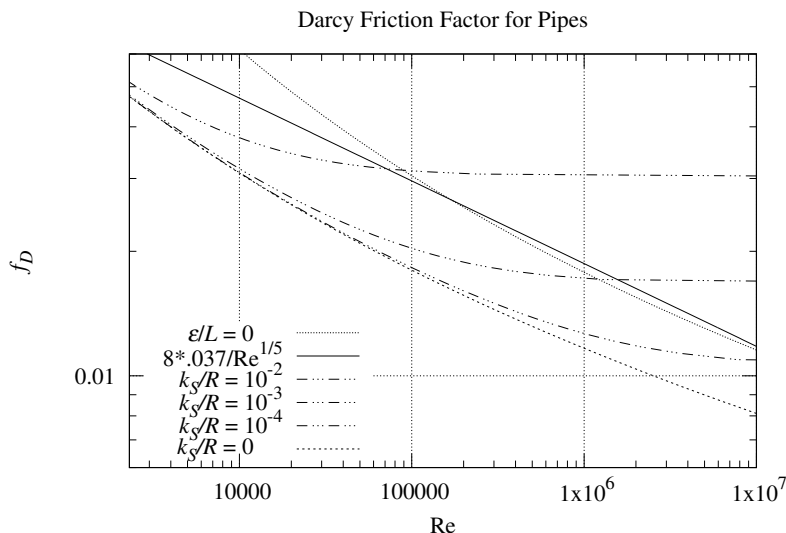


Figure 1

When the sand-roughness $k_S > 0$, $f_D(\text{Re})$ is asymptotically constant as Re increases, and Nu in the Chilton and Colburn J-factor analogy (3) is proportional to Re (versus $\text{Re}^{4/5}$ in smooth pipes).

Lienhard and Lienhard[6] teach that a very thin viscous sublayer “is responsible for a major fraction of the thermal resistance of a turbulent boundary layer.”

At the scale of the viscous sublayer, the inner radius curvature (being perpendicular to the flow) in a large diameter pipe should be indistinguishable from a flat plate. Because most of the convective thermal resistance occurs close to the surface of a pipe or plate, it is reasonable to expect the turbulent correlations for pipe and plate to be related.

The solid trace in Figure 1 is correlation (5) for skin-friction of a smooth plate. It does not lie near the curve for a smooth surface $k_S/R = 0$; but roughly parallels it in the range $10^5 < \text{Re} < 10^7$.

Although it must have the correct relation to dimensions and parameters, the scale of characteristic-length is otherwise a matter of convention (both radius and diameter have been used for pipes). The forced-convection correlations are usually monomials in Re and scale easily. With the characteristic-length of a pipe being perpendicular to the direction of flow and the characteristic-length of a plate being in the direction of flow, it is not unreasonable that scaling may be necessary in order to make correspondences between them.

Scaling the characteristic-length $R \rightarrow L/9.5$ and $Re \rightarrow Re_F/9.5$ in the Colebrook-White equation causes the scaled smooth convection curve ($\varepsilon/L = 0$) to approximate correlation (5) in Figure 1 above $Re = 10^5$. If the mean height-of-roughness ε , which is perpendicular to the characteristic-length for both pipes and plates, can be correctly scaled, the result may predict convection for rough plates.

Doubts about how to scale the roughness in the Colebrook-White equation motivated the construction of an apparatus designed to measure rough plate convection. The resulting measurements were well matched by scaling the height-of-roughness $k_S \rightarrow \varepsilon 7.41/9.5$ (such that the first term of the argument to \log_{10} becomes ε/L). This scaled Colebrook-White equation is (7):

$$\frac{1}{\sqrt{f_D}} = -2 \log_{10} \left(\frac{\varepsilon}{L} + \frac{9.5 \cdot 2.51}{Re_F \sqrt{f_D}} \right) \quad (7)$$

Its asymptote as $Re_F \rightarrow \infty$ is:

$$\frac{1}{\sqrt{f_D}} = -2 \log_{10} \frac{\varepsilon}{L} \quad f_D = \frac{1}{4 \left[\log_{10} \frac{\varepsilon}{L} \right]^2} \quad f_c = \frac{1}{16 \left[\log_{10} \frac{\varepsilon}{L} \right]^2} \quad (8)$$

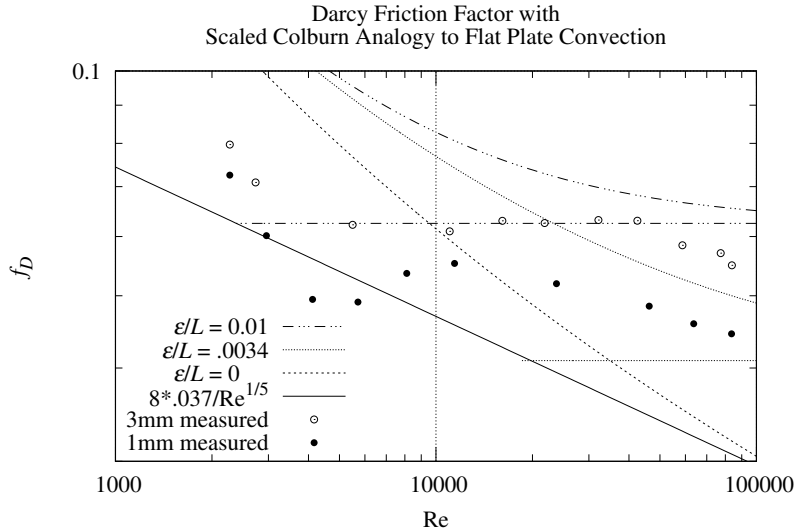


Figure 2

Most of the “3 mm measured” convection points lie close to the $\varepsilon/L = 0.01$ asymptotic value, not the $\varepsilon/L = 0.01$ curve. It is acknowledged in both Prandtl and Schlichting[2] and Afzal et al[7] that a single roughness parameter is not sufficient to characterize its behavior.

Afzal et al[7] shows a family of curves (monotonic to inflectional) controlled by two parameters. The lower bound of the whole family is smooth pipe skin-friction. But the (3 mm roughness) measured points lie on neither monotonic nor inflectional curves; and are not bounded by the smooth plate skin-friction ($\varepsilon/L = 0$).

This problem is also clearly seen in convection. The scaled Colburn analogy asymptote (9) is the result of combining the scaled Colebrook-White equation asymptote (8) with the Chilton and Colburn J-factor analogy (3):

$$\text{Nu}_F = \frac{\text{Re}_F \text{Pr}^{1/3}}{32 \left[\log_{10} \frac{\varepsilon}{L_F} \right]^2} \quad (9)$$

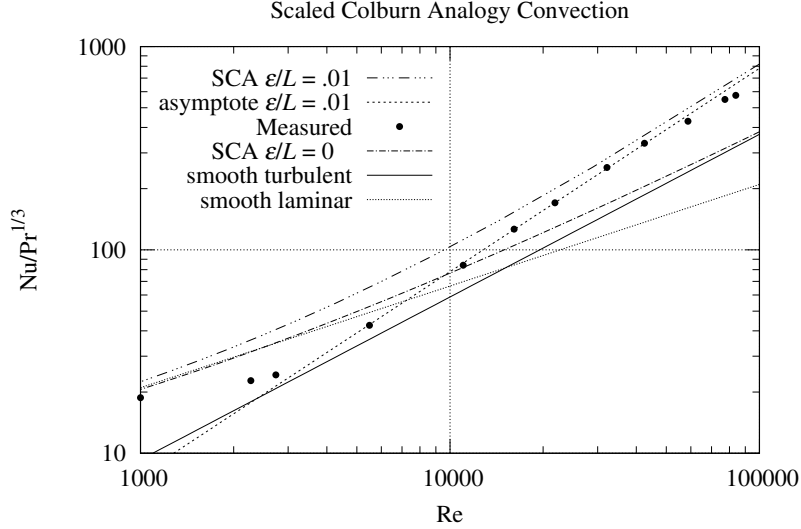


Figure 3

Measurements displayed in Figure 3 show that rough surface convection is a linear function of Re_F down to $\text{Re}_F = 5490$. Compensating for mixed convection, it could be linear to $\text{Re}_F = 2383$, the intercept for smooth turbulent and $\varepsilon/L = 0.01$ asymptotes. Figure 3 shows that scaled Colburn analogy convection (top trace) is not linear. Its asymptote (9) is a much better fit to the data. Correlation (9) corresponds to the “fully-developed roughness” region of Prandtl and Schlichting, but extends to much lower Reynolds numbers.

The deviation of the measured data from correlation (9) at $\text{Re} < 5000$ can be accounted for by the mixing of natural and forced convection. The deviation at $\text{Re} > 50000$ is addressed in Section 5.

Although successfully modeled by Section 5, the points for the 1 mm plate are not near the $\varepsilon/L = 0.0034$ curve or its asymptotic value in Figure 2 because most of the forced convection measured is smooth-turbulent (with two different characteristic-lengths). The influence of rough-turbulence is seen in the measurements below the $8 * .037/\text{Re}^{1/5}$ trace. Were natural convection not obscuring measurements, it is likely that the region of flat rough-turbulence would extend below the smooth-turbulence asymptote. This indicates that some assumption underlying the Colebrook-White equation (6) is not in effect for rough plates. So this proposed pipe-plate analogy is flawed, but its asymptote (9) matches the 3 mm roughness experiments well.¹

When ε of the plate was reduced from 3 mm to 1 mm, the repeat length in the direction of flow S_S was not similarly scaled. The skin-friction traces for plates with self-similar roughness should be level down to scales of peak height comparable to the admissible height of roughness (see Section 7).

Natural convection prevents investigation of the forced smooth-rough turbulent transition by heat transfer; measurement of skin-friction drag would be a better methodology for lower Reynolds number ranges.

¹ The scaled Colebrook-White asymptote (8) is simpler than the skin-friction formulas from Prandtl and Schlichting (1) and Mills and Hang (2). It was unexpected that the base ten logarithm in correlation (8) would require no coefficient or offset.

5. Rough to Smooth Turbulence Transition

The roughness of the bi-level plate is not self-similar; it exhibits different convection behaviors at different scales. The slope of the upper end of both curves in Figure 5 is 4/5, but with a magnitude possible only if operating with a much shorter characteristic-length than the plate's $L_F = 0.305$ m.

At the leading edge of the plate, the smooth-turbulent boundary-layer depth would be much smaller than the height-of-roughness; so fully rough convection (9) applies. The boundary-layer depth increases with distance x from the leading edge:

$$\delta_{tur}(x) = \frac{0.37x}{\text{Re}_x^{1/5}} = 0.37x^{4/5} \left(\frac{L}{\text{Re}} \right)^{1/5} = 0.37L \frac{\text{Re}_x^{4/5}}{\text{Re}} \quad (10)$$

Solving for Re_x where $\delta_{tur} = \varepsilon_{pv}$, the peak-to-valley height:

$$\text{Re}_x = \left(\frac{\varepsilon_{pv}}{L} \frac{\text{Re}}{0.37} \right)^{5/4}$$

Around

$$\text{Re}_x > \frac{\varepsilon_{pv}}{L_S} \left(\frac{\varepsilon_{pv}}{L} \frac{121 \times 10^3}{0.37} \right)^{5/4} \quad (11)$$

the flow transitions to a regime consisting of smooth turbulent convection (4) from the channels between posts at scale L_F and smooth turbulent convection (4) from the post at scale $L_S = 8.3$ mm, the length of the post in the direction of flow.

Where $S_S = L/26$ is the post center spacing, the longitudinal (parallel to flow) channels between the posts have convection:

$$\text{Nu}_C / \text{Pr}^{1/3} = \frac{S_S - L_S}{S_S} \cdot 0.037 \cdot \text{Re}^{4/5} \quad (12)$$

The top of the posts occupy half (L_S^2/S_S^2) of the plate area; their convection is:

$$\text{Nu}_T / \text{Pr}^{1/3} = \frac{L_S^2}{S_S^2} \left(\frac{L_F}{L_S} \right)^{1/5} \cdot 0.037 \cdot \text{Re}^{4/5} \quad (13)$$

The $(L_F/L_S)^{1/5}$ factor converts the characteristic-length from L_S to L_F .

Both post sides parallel to the flow also experience smooth turbulent convection at scale $L_S = 8.3$ mm, but because the sides are within the channel's boundary layer, T_F , V and Re are not constant with elevation. The channel velocity profile provides velocity as a function of elevation y , boundary layer depth δ , and free stream velocity V :

$$\frac{v}{V} = \begin{cases} (y/\delta)^{1/7} & \text{when } y \leq \delta; \\ 1, & \text{otherwise.} \end{cases}$$

By analogy with the derivation of the thermal profile for laminar flow from Lienhard and Lienhard[6], the turbulent thermal profile would be:

$$\frac{T - T_w}{T_\infty - T_w} = \begin{cases} (y/\delta_t)^{1/7} & \text{when } y \leq \delta_t; \\ 1, & \text{otherwise.} \end{cases} \approx \begin{cases} \left(y / \left(\delta \text{Pr}^{-1/3} \right) \right)^{1/7} & \text{when } y \leq \delta; \\ 1, & \text{otherwise.} \end{cases}$$

The temperature profile will affect side convection by a factor of approximately $\text{Pr}^{1/21} (y/\delta)^{1/7}$ when $y \leq \delta$; and 1 otherwise. In air, $\text{Pr}^{1/21}$ is a reduction by 1.5% (for the post sides convection only).

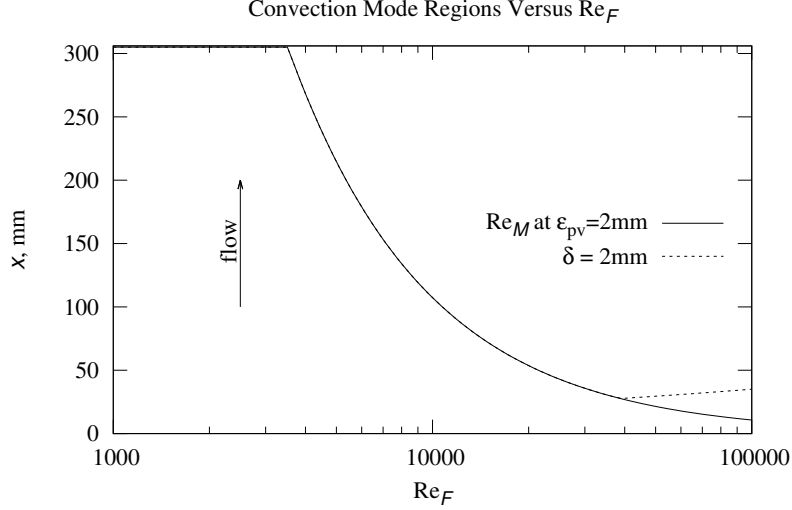


Figure 4

Each vertical slice of Figure 4 represents the regions of convection on the surface of the 1 mm roughness plate at the indicated value of Re_F . The entire surface is in rough turbulent convection of correlation (9) below the Re_M trace where (11) is not satisfied. Above the Re_M trace, the convection is modeled as a combination of channel (12), post-top (13), and post-side (14) convection. When Re_F is larger than 40000, there is a small region where the channel boundary-layer height is smaller than the post side height $\varepsilon_{pv} = 2$ mm. Post side convection from this region was modeled, but its effect on total convection was negligible. For simplicity, the post side model uses formula (14) for all post side convection.

The convection for a vertical slice of the post side is:

$$\begin{aligned}
 \chi(x) &= \frac{0.037}{\varepsilon_{pv}} \int_0^{\varepsilon_{pv}} \left(\frac{y}{\delta_F(x) \text{Pr}^{-1/3}} \right)^{1/7} \left(\text{Re}_x \left(\frac{y}{\delta_F(x)} \right)^{1/7} \right)^{4/5} dy \\
 &= \frac{0.037 \text{Pr}^{1/21}}{\varepsilon_{pv}} \int_0^{\varepsilon_{pv}} \left(\frac{y}{0.37x^{4/5}} \left(\frac{\text{Re}}{L} \right)^{1/5} \right)^{1/7} \left(\frac{\text{Re} x}{L} \left(\frac{y}{0.37x^{4/5}} \left(\frac{\text{Re}}{L} \right)^{1/5} \right)^{1/7} \right)^{4/5} dy \\
 &= 0.038 \frac{\text{Re}^{149/175} \text{Pr}^{1/21} x^{113/175} \varepsilon_{pv}^{9/35}}{L^{158/175}}
 \end{aligned}$$

The convection from a row of post sides in line with the flow is:

$$\begin{aligned}
 \text{Nu}_S / \text{Pr}^{1/3} &= 2 \frac{\varepsilon_{pv} L_S}{S_S^2} \left(\frac{L_F}{L_S} \right)^{1/5} \frac{1}{L_F} \int_0^{L_F} \chi(\varepsilon_{pv}) dx \\
 &= 2 \frac{\varepsilon_{pv} L_S}{S_S^2} \left(\frac{L_F}{L_S} \right)^{1/5} 0.0231 \text{Pr}^{1/21} \left(\frac{\varepsilon_{pv}}{L_F} \right)^{9/35} \text{Re}^{149/175}
 \end{aligned} \tag{14}$$

Integrating the local convections for correlations (9), (12), (13), and (14) over distance:

$$\begin{aligned}
 \text{Re}_M &= \min \left(\text{Re}_F, \frac{\varepsilon_{pv}}{L_S} \left(\frac{\varepsilon_{pv} \text{Re}_t}{L} 0.37 \right)^{5/4} \right) \quad \text{Re}_t = 121 \times 10^3 \\
 \text{Nu}_F / \text{Pr}^{1/3} &= \frac{\text{Re}_M}{32 \left[\log_{10} \frac{\varepsilon}{L_F} \right]^2} + \left[\frac{S_S - L_S}{S_S} + \frac{L_S^2}{S_S^2} \left(\frac{L_F}{L_S} \right)^{1/5} \right] 0.037 \left(\text{Re}_F^{4/5} - \text{Re}_M^{4/5} \right) \\
 &\quad + 2 \frac{\varepsilon_{pv} L_S}{S_S^2} \left(\frac{L_F}{L_S} \right)^{1/5} 0.0231 \text{Pr}^{1/21} \left(\frac{\varepsilon_{pv}}{L_F} \right)^{9/35} \left(\text{Re}_F^{149/175} - \text{Re}_M^{149/175} \right)
 \end{aligned} \tag{15}$$

The constant Re_t adds a degree of freedom to the plate model; but Figure 8 shows that 121000 fits both 3 mm roughness and 1 mm roughness data-sets within their estimated uncertainties below $Re=80000$. Figure 9 shows that the percentage discrepancy from the mixed model for 3 mm roughness is within $\pm 2\%$ below $Re=80000$.

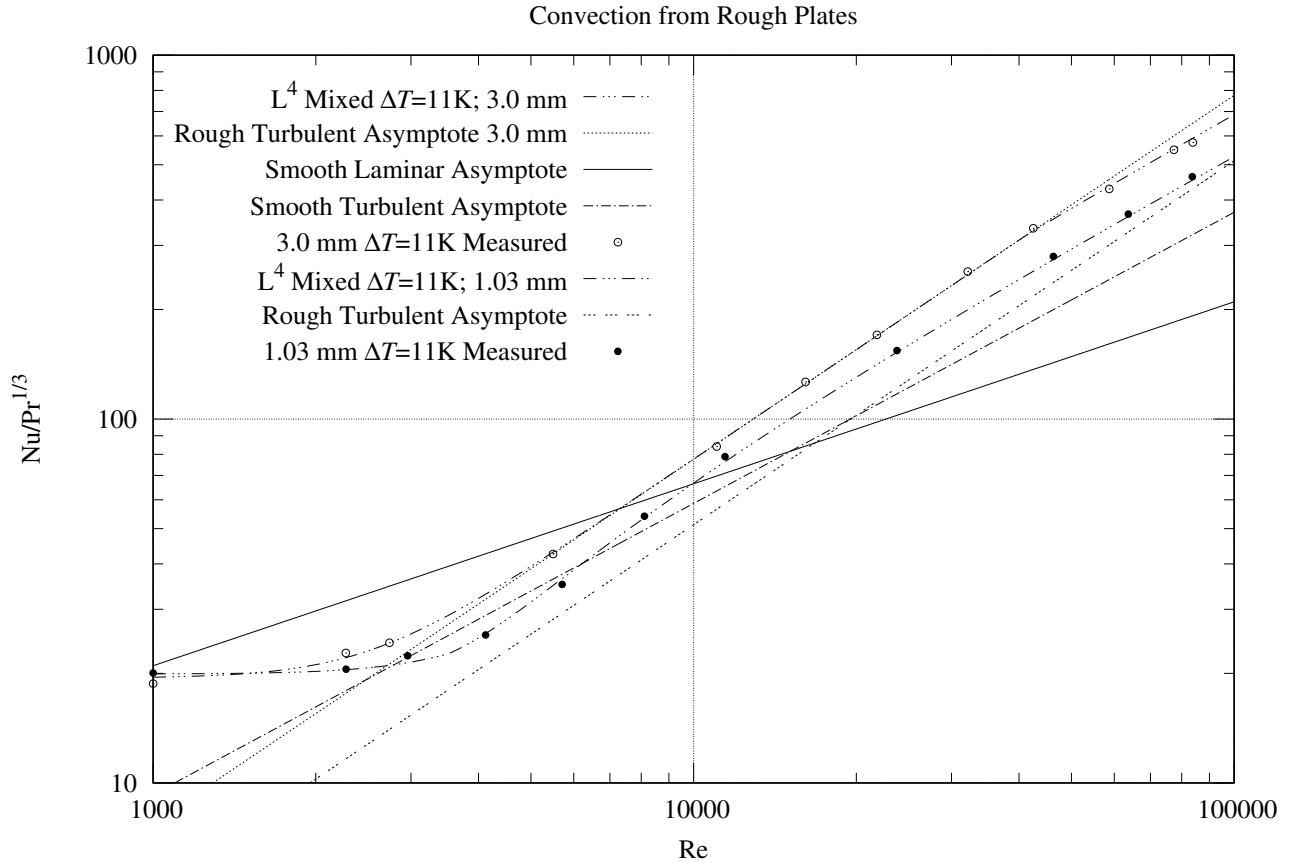


Figure 5

While the L^4 Mixed and Rough Turbulent Asymptote traces for 3 mm roughness are close in Figure 5, those traces for 1 mm roughness are not. This is because when ε of the plate was reduced from 3 mm to 1 mm, L_S was not similarly scaled.

6. Sand Roughness

Modeling sand grains as unit radius spheres glued to the plate surface in a square array and modeling the space not covered by a sphere as glue of height $0 \leq \bar{y} \leq 1$, the mean height of the enclosing square cell of area A containing a unit sphere is:

$$\bar{y} = \left(\int_0^1 2\pi x (\sqrt{1-x^2} + 1) dx + (A - \pi)\bar{y} \right) / A = \left(\frac{5}{3}\pi + (A - \pi)\bar{y} \right) / A$$

The arithmetic-mean height-of-roughness R_a and the root-mean-squared height-of-roughness R_q are:

$$2R_a = \left(\int_0^1 2\pi x |\sqrt{1-x^2} + 1 - \bar{y}| dx + (A - \pi) |\bar{y} - \bar{g}| \right) / A$$

$$2R_q = \sqrt{\left(\int_0^1 2\pi x (\sqrt{1-x^2} + 1 - \bar{y})^2 dx + (A - \pi) (\bar{y} - \bar{g})^2 \right) / A}$$

For glue level $1 < \bar{g} < 2$, the grains are more than 50% submerged. Let $x_g = \sqrt{(1 - (\bar{g} - 1)^2)} = \sqrt{2\bar{g} - \bar{g}^2}$ be the radius of the glue opening through which the sphere is exposed. The mean height of the enclosing square cell of area A containing a unit sphere is then:

$$\bar{y} = \left(\int_0^{x_g} 2\pi x (\sqrt{1-x^2} + 1) dx + (A - \pi x_g^2) \bar{y} \right) / A = \left(\frac{4 + 3\bar{g}^2 - 2\bar{g}^3}{3} \pi + (A - \pi x_g^2) \bar{y} \right) / A$$

The arithmetic-mean height-of-roughness R_a and the root-mean-squared height-of-roughness R_q are:

$$2R_a = \left(\int_0^{x_g} 2\pi x |\sqrt{1-x^2} + 1 - \bar{y}| dx + (A - \pi x_g^2) |\bar{y} - \bar{g}| \right) / A$$

$$2R_q = \sqrt{\left(\int_0^{x_g} 2\pi x (\sqrt{1-x^2} + 1 - \bar{y})^2 dx + (A - \pi x_g^2) (\bar{y} - \bar{g})^2 \right) / A}$$

Figure 6 shows the conversion factor from ε to k_S as a function of relative glue thickness.

Sand-Roughness k_S per Height-of-Roughness ε vs. Glue Thickness and Cell Area A

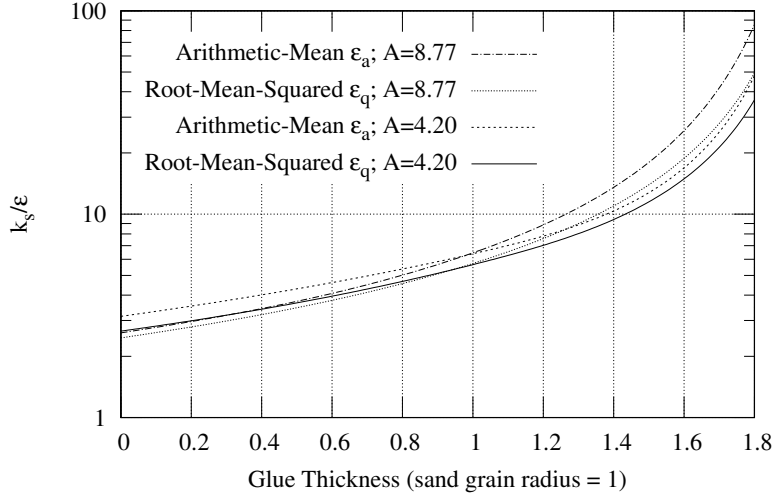


Figure 6

In order to compare the Prandtl and Schlichting[2] formula (1) with formula (8) of present work, different k_S/ε conversion factors (and relative glue thicknesses) must be used at large and small k_S values.

The unit cell area for the larger grains is 4.2. With $L/\varepsilon = 150$, compare $4c_f$ for $L/k_S = R_a L/\varepsilon$ in Table 2 and $L/k_S = R_q L/\varepsilon$ in Table 3 with $f_D = 0.0528$ calculated from the scaled Colebrook-White asymptote (8):

\bar{g}	\bar{y}	$1/R_a$	L/k_S	$4c_f$
0.00	1.25	3.14	47.7	0.088
0.70	1.42	4.97	30.2	0.105
1.00	1.50	6.38	23.5	0.117

Table 2 Average roughness R_a versus large-grain sand-roughness k_S

\bar{g}	\bar{y}	$1/R_q$	L/k_S	$4c_f$
0.00	1.25	2.66	56.4	0.082
0.87	1.47	4.98	30.1	0.105
1.00	1.50	5.64	26.6	0.111

Table 3 RMS roughness R_q versus large-grain sand-roughness k_S

$f_D = 0.0528$ is out of the range of possible $4c_f$ values for arithmetic-mean and RMS roughness with $\bar{g} \geq 0$. However, there are values of $4c_f/2$ which are within range for both RMS and arithmetic-mean roughness.

A factor of 2 is introduced in the last step of Prandtl and Schlichting’s paper[2]. While it is justified for the local coefficient of resistance, the reason for its presence in the total coefficient of resistance is not obvious. In their example of the use of their formula, Mills and Hang[4] divide C_D by 2.

Half the $4c_f$ value from the $\bar{g} = 0.70$ row in Table 2 matches $f_D = 0.0528$, as does the $\bar{g} = 0.87$ row in Table 3, for arithmetic-mean and RMS height-of-roughness respectively.

The unit cell area for the smaller grains is 8.77. The largest pipe which Nikuradse tested had a diameter of 0.101 m. With a coating made from the smallest sand grain size (.01 cm), $L/k_S = 1014$ and the corresponding $f_D = 0.0277$. As before, there is no glue level $\bar{g} \geq 0$ whose $4c_f$ matches f_D , but half of $4c_f$ does match at $\bar{g} = 0.90$ and $\bar{g} = 0.99$ in Tables 4 and 5.

\bar{g}	\bar{y}	$1/R_a$	L/k_S	$4c_f$
0.00	0.60	2.61	388.6	0.044
0.90	1.17	5.65	179.4	0.055
1.50	1.57	17.98	56.4	0.082

Table 4 Average roughness R_a versus small-grain sand-roughness k_S

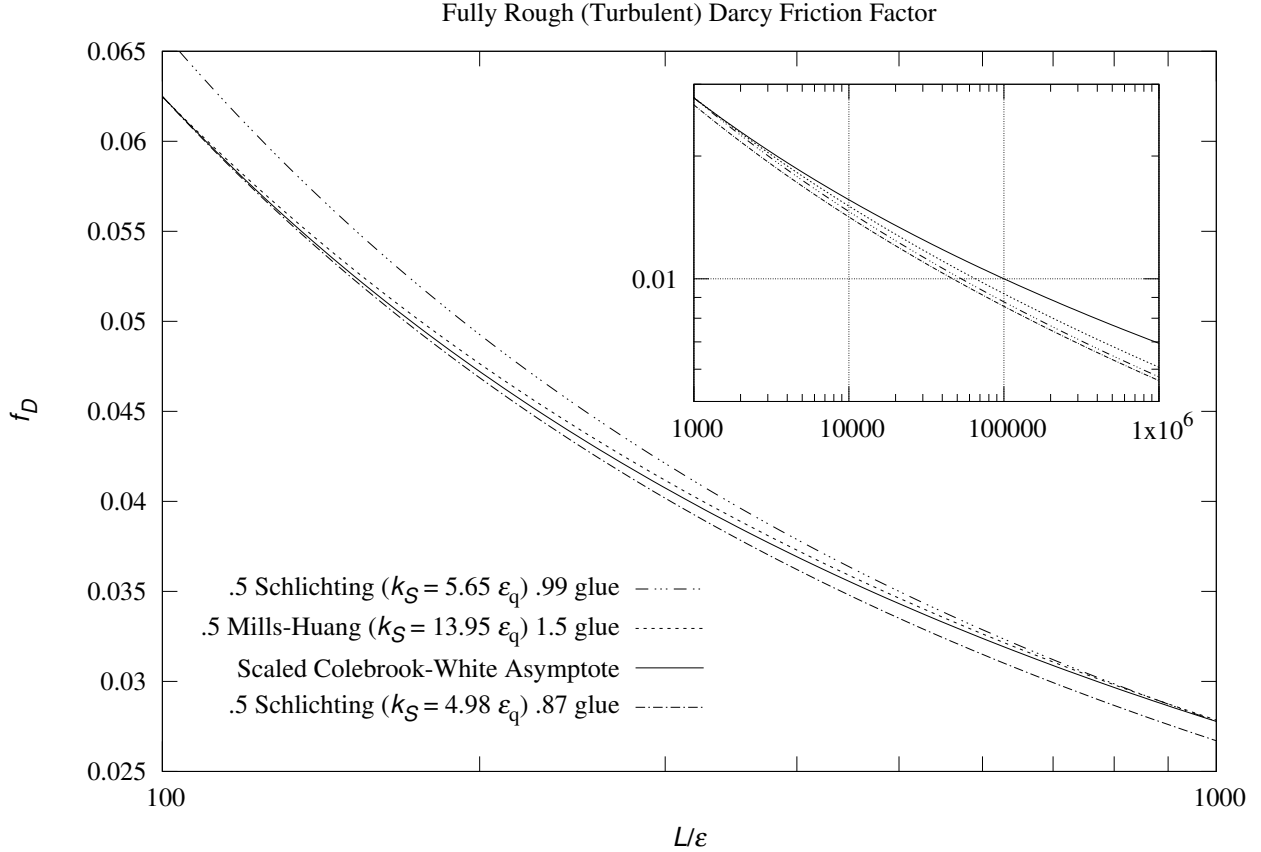
\bar{g}	\bar{y}	$1/R_q$	L/k_S	$4c_f$
0.00	0.60	2.46	411.4	0.043
0.99	1.23	5.65	179.4	0.055
1.50	1.57	13.95	72.7	0.075

Table 5 RMS roughness R_q versus small-grain sand-roughness k_S

Afzal et al in *Turbulent flow in a machine honed rough pipe for large Reynolds numbers: General roughness scaling laws*[7] fit 5.333 for the RMS to sand-roughness conversion factor and 6.45 for the arithmetic-mean to sand-roughness conversion factor. The mean of the $1/R_q$ values 4.98 and 5.65 is within 1% of 5.333 (and not close to 6.45). This is strong evidence that RMS height-of-roughness is the true metric for surface roughness in the scaled Colebrook-White asymptote (8).

In *Skin-friction behavior in the transitionally-rough regime*[8], Flack et al measure skin-friction from grit-blasted surfaces. They find “The root-mean-square roughness height (k_{rms}) is shown to be most strongly correlated with the equivalent sand roughness height (k_S) for the grit-blasted surfaces.”

Figure 7 shows that the Mills-Hang formula (2) is nearly coincident with the Colebrook-White asymptote (8) over the range $100 < L/\varepsilon < 1000$; so it is an improvement over Prandtl and Schlichting’s correlation (1). At $L/\varepsilon > 1000$, the inset in Figure 7 shows that both suffer from the scale error discussed in Section 2, growing to -13% and -18% relative to the scaled Colebrook-White asymptote (8) at $L/\varepsilon = 10^6$.



7. Admissible Roughness

“The amount of roughness which is considered “admissible” in engineering applications is that maximum height of individual roughness elements which causes no increase in drag compared with a smooth wall.”² Schlichting[3] develops a formula for k_{adm} from its Fig. 21.9. (Resistance formula of sand-roughened plate; coefficient of *total* skin friction):

$$U_\infty k_{adm} / \nu = 100 \quad (16)$$

A footnote states “The estimates performed in this section make no distinction between the equivalent sand height, k_S , and the actual height, k , of a protuberance.” In the Section 6 model of sand-roughness, the protuberance height is $(1 - \bar{g}/2)k_S$. For Nikuradse’s large grains that is $0.57 k_S$; for small grains it is $0.51 k_S$. So equation (16) overestimates the admissible-roughness height.

The admissible-roughness threshold does not occur in the “fully-developed roughness” region (Prandtl and Schlichting[2]) which contains all the Convection Machine measurements. However, these measurements can be used to develop an upper bound for admissible-roughness.

For a given RMS roughness R_q , the equal-area bi-level plate has the smallest possible $k = 2R_q$; while large-grain sand-roughness would have $k = 0.57 \cdot 5.333R_q = 3.0R_q$ and small-grain $k = 0.51 \cdot 5.333R_q = 2.7R_q$.

The basis for equation (16) is that $U_\infty k_S / \nu = \text{Re } k_S / L$ is nearly invariant at the intercepts of the constant k_S / L and $k_S = 0$ curves at Re from 10^5 to 10^8 . For the 1.03 mm trace in Figure 5, this would be the point below which the slope of measured $\text{Nu}/\text{Pr}^{1/3}$ is 4/5. Natural convection obscures the slope below $\text{Re}=4419$; so 4419 is an upper bound. This upper bound for k is a significant reduction from equation (16):

$$R_q \frac{U_\infty}{\nu} = R_q \frac{\text{Re}}{L} < 15 \quad k \frac{U_\infty}{\nu} = k \frac{\text{Re}}{L} < 30 \quad k < 30 \frac{\nu}{U_\infty} = 30 \frac{L}{\text{Re}} \quad (17)$$

² This definition does not imply that roughness always causes an increase in drag; for example in Figure 5 the 1 mm roughness curve is less than the smooth-turbulent asymptote from $3000 < \text{Re} < 7000$.

8. Forced Convection Results

Figure 8 compares the measurements for the downward-facing plates with equations (15) and (9) and their predicted uncertainties calculated for each measurement. Below $Re=5000$ the curves for equation (15) are corrected for mixed convection, as described in *Turbulent Mixed Convection from an Isothermal Plate*[9].

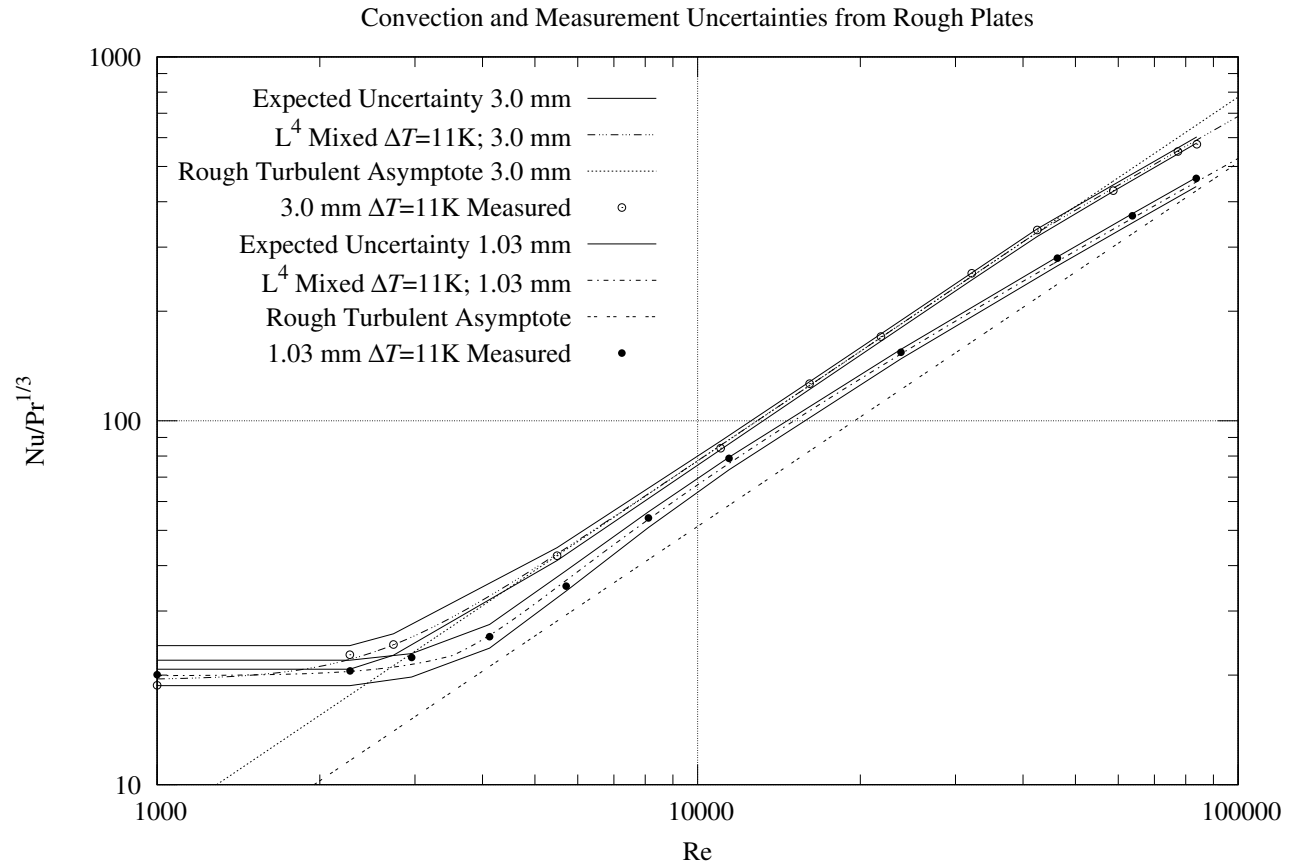


Figure 8

Figure 9 shows that the percentage discrepancy from the mixed model is within $\pm 2\%$ below $Re=80000$.

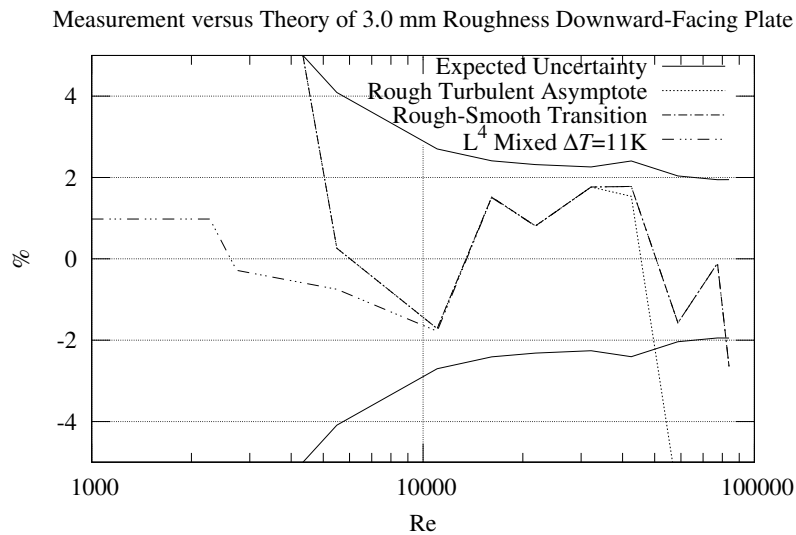


Figure 9

9. Directions for Further Work

The Rough to Smooth Turbulence Transition model of Section 5 should not be necessary if the roughness of the plate were self-similar. But machining a self-similar rough surface from metal is difficult. A 3D-printer can create self-similar rough surfaces easily. Furthermore, it can create plates with self-similar roughness on both sides, eliminating the complications and uncertainties of the back and side models.

Convection measurements require the plate to have high thermal conductivity. The alternative is to measure (skin-friction) drag of the plate in the wind-tunnel. Work is underway to equip the Convection Machine wind-tunnel with a 0.1 N (10 g) load-cell to measure drag. Drag measurements will be made without heating, enabling the metal plate to be replaced with plastic ones from the 3D-printer. An added benefit of drag measurements is that natural convection will no longer obscure measurements made at $Re < 5000$.

10. Conclusions

The current practice for fluid-dynamics on rough surfaces involves estimating sand-roughness, a non-traceable unit which has a non-linear relationship to RMS height-of-roughness.

Convection measurements of plates having precisely machined height-of-roughness drove discovery of new formulas for skin-friction and forced convection using RMS height-of-roughness ε_q instead of sand-roughness.

$$f_c = \frac{1}{16 [\log_{10} \frac{\varepsilon_q}{L}]^2} \quad Nu = \frac{Re Pr^{1/3}}{32 [\log_{10} \frac{\varepsilon_q}{L}]^2}$$

The experiments performed with a 1.03 mm RMS height-of-roughness plate provide an upper bound for admissible roughness in terms of peak-to-valley height instead of sand-roughness. The maximum height of admissible roughness k is no more than:

$$k < 30 \frac{L}{Re} = 30 \frac{\nu}{U_\infty}$$

Acknowledgments

Thanks to John Cox and Doug Ruuska for machining the plate. Thanks to Martin Jaffer and Roberta Jaffer for their assistance and problem-solving suggestions.

11. References

- [1] A. Jaffer. Convection measurement apparatus and methodology, 2018. [Online; accessed 30-August-2018].
- [2] L. Prandtl and H. Schlichting. *The Resistance Law for Rough Plates*. Translation (David W. Taylor Model Basin). Navy Department, the David W. Taylor Model Basin, 1934. Translated 1955 by P.S. Granville.
- [3] Hermann Schlichting, Klaus Gersten, Egon Collaborateur. Krause, Herbert Collaborateur. Oertel, and Katherine Mayes. *Boundary-layer theory*. Springer, Berlin, Heidelberg, Paris, 2000. Corrected printing 2003.
- [4] A. F. Mills and Xu Hang. On the skin friction coefficient for a fully rough flat plate. *J. Fluids Eng*, 105(3):364–365, 1983.
- [5] M. M. Pimenta, R. J. Moffat, and W. M. Kays. *The Turbulent Boundary Layer: An Experimental Study of the Transport of Momentum and Heat with the Effect of Roughness*. Department of Mechanical Engineering, Stanford University, 1975.
- [6] J.H. Lienhard IV and J.H. Lienhard V. *A Heat Transfer Textbook*. Phlogiston Press, Cambridge, MA, 4th edition, 2016. Version 2.04.
- [7] Noor Afzal, Abu Seena, and A. Bushra. Turbulent flow in a machine honed rough pipe for large reynolds numbers: General roughness scaling laws. *Journal of Hydro-environment Research*, 7(1):81–90, 2013.
- [8] Karen A Flack, Michael P Schultz, Julio M Barros, and Yechan C Kim. Skin-friction behavior in the transitionally-rough regime. *International Journal of Heat and Fluid Flow*, 61:21–30, 2016.
- [9] A. Jaffer. Turbulent mixed convection from an isothermal plate, 2018. [Online; accessed 30-August-2018].